Journal of Applied Polymer Science

P3HT : PCBM Solar Cells—The Choice of Source Material

Annie Ng,[1] Xiang Liu,[1] Wai Yan Jim,[1] Aleksandra B. Djurišić,[1] Kin Cheung Lo,[2] Sheung Yin Li,[2] Wai Kin Chan[2]

[1]Department of Physics, The University of Hong Kong, Pokfulam Road, Hong Kong

[2]Department of Chemistry, The University of Hong Kong, Pokfulam Road, Hong Kong

Correspondence to: A. B. Djurišić (E-mail: dalek@hku.hk)

ABSTRACT: Bulk heterojunction solar cells based on P3HT : PCBM blend films are among the most intensively studied polymer solar cells. In spite of that, there is a huge variation of reported efficiencies in the literature, even for same device architectures and film preparation procedures. Here we investigated the influence of starting properties of P3HT and PCBM (different suppliers) on blend film morphology and device performance. We found that there was a strong dependence of the film morphology and device performance on the source of chemicals used. Both P3HT and PCBM affected the results, and higher nominal purity did not necessarily result in better device performance. The dependence of the film morphology and device performance on the properties of P3HT and PCBM is discussed in detail. © 2013 Wiley Periodicals, Inc. J. Appl. Polym. Sci. 000: 000–000, 2013

KEYWORDS: films; optical and photovoltaic applications; blends

Received 7 May 2013; accepted 17 July 2013; Published online

DOI: 10.1002/app.39776

INTRODUCTION

Among various bulk heterojunction material combinations, poly(3-hexyl thiophene) (P3HT): 1-(3-methoxycarbonyl)-propyl-1-phenyl-[6,6] C_{61} (PCBM) is very commonly investigated.[1–40] Over a thousand of research articles reporting on P3HT : PCBM bulk heterojunctions were published between 2002 and 2010.[1] However, although this material system can achieve efficiencies up to ~5%,[31,32] average efficiency reported in 2010 was only ~3% and efficiencies below 0.5% were still reported.[1] This situation has not significantly changed in 2011 and 2012, with efficiencies below 0.5–1.5% still reported for some devices,[10,24] and efficiencies below 3% under optimal preparation conditions still commonly found,[10,15,17,18,30] with very few devices approaching or exceeding 4%.[14,21,26,35]

Possible reasons for the reported wide range of efficiency values of P3HT : PCBM bulk heterojunctions in the literature are variations in the purity of chemicals used, as well as regioregularity (RR) and molecular weight (M_w) of P3HT.[1] Naturally, other factors such as solvent used, ratio of P3HT to PCBM, annealing conditions, film thickness, and device architecture also affect the cell performance.[1] Furthermore, obtained results can depend on various processing factors, such as the age of blend solution and mixing conditions.[16] Nevertheless, there is a large dispersion of the reported values in the literature for devices with the same architecture, film thickness, and preparation conditions (solvent, P3HT : PCBM ratio, annealing), which could only occur due to differences in material properties of P3HT and PCBM. However, in review of the literature on this type of solar cells the effect of starting materials purity has not been investigated due to variations in impurities, M_w, and polydispersity index (PDI) for different suppliers or different batches of material.[1] However, it was found that the miscibility of P3HT and PCBM was dependent on the supplier even for similar values of M_w and PDI.[16] Consequently, it was proposed that the information provided by the manufacturer on PDI, M_w, RR, and purity is incomplete (or possibly inaccurate) information for determining device morphology and its photovoltaic performance.[16]

In addition to the device performance, surface morphology and charge transport were found to be dependent on the P3HT molecular weight.[9] The differences in the performance of cells prepared with different molecular weight of P3HT were attributed to differences in bulk heterojunction morphology due to different solubility of P3HT (higher M_w material is less soluble), as well as different rates of diffusion of PCBM during annealing (low M_w, high diffusion rate of PCBM).[5] Low molecular weight can also have detrimental effects on intermolecular ordering, resulting in inferior device perofrmance.[6] Molecular weight of

Additional Supporting Information may be found in the online version of this article.

P3HT was also proposed to affect crystallization behavior.[8] All these factors could affect the morphology of the blend film. The optimal morphology of a P3HT : PCBM blend consists of PCBM aggregates and P3HT crystallites both with domain sizes smaller than 20 nm, which are contained in a matrix consisting of mixed P3HT and PCBM.[3,14] Optimal morphology needs to provide efficient percolation paths for electron and hole transport, as well as efficient exciton dissociation and low recombination losses.[1] Relatively larger P3HT domains with low disorder were reported to be favorable for charge generation and extraction, and consequently for efficient photovoltaic performance.[15]

Therefore, it is important to study the influence of the material properties (purity, M_w, and PDI) on the bulk heterojunction morphology and the device performance. Obtaining this information is essential for improving the reproducibility of devices prepared for a certain material combination, such as P3HT : PCBM. A large number of research laboratories relies on commercial material suppliers for the polymers and fullerene derivatives for photovoltaics research. Consequently, it is important to systematically examine variation, if any, of blend film properties and photovoltaic performance for different source material suppliers, as well as different lot numbers and ambient storage exposure times. Adhesion of the films to the substrate (and/or metal electrode) can also be dependent on the source material used, which can affect the stability of the cells, as well as the ability to examine morphology and/or optical properties of annealed devices by peeling off the top electrode,[38] for example. We have selected two different suppliers for both P3HT and PCBM, and for one of the suppliers two different lot numbers were considered. All devices were prepared under the same conditions (solution preparation, solvent use, concentration, P3HT : PCBM ratio) and with the same simple device architecture. We have selected to study devices with P3HT : PCBM ratio 1 : 0.8, prepared from chlorobenzene solutions as a very commonly used preparation procedure. The device architecture was glass/indium tin oxide (ITO)/poly(3,4-ethylenedioxy thiophene) : poly (styrene sulfonate) (PEDOT:PSS)/P3HT:PCBM/Al. Different annealing conditions were tried for two different sources of P3HT in order to not only compare devices prepared under the same conditions but also establish what is the best efficiency that can be achieved for a certain combination of two suppliers of P3HT and PCBM. Surprisingly, we found that not only P3HT but also PCBM source and purity had a significant effect on bulk heterojunction morphology and solar cell performance.

EXPERIMENTAL DETAILS

P3HT was obtained from two different sources: P200 P3HT (Rieke Metals Lot#2010-A6–7; $M_w = 21{,}809$ g/mol; PDI 1.63; RR 95.1%), labeled R-P3HT and RN-P3HT (RN indicates same the lot number, but freshly opened bottle) and ADS P3HT (American Dye Source, Lot#10H028A; M_w: 30,000 g/mol; PDI: 2.9; RR: 95–98% and Lot#11G032A M_w: 31,000 g/mol; PDI: 1.8; RR: 95–98%), labeled A1-P3HT and A2-P3HT, respectively. For both sources M_w exceeds 10,000 g/mol, which was found to be necessary to achieve higher efficiencies.[2,6,7] PCBM was also obtained from two sources: Nano C PCBM (BJ110729, Purity: 99.5%), labeled N-PCBM and NN-PCBM (NN indicates the same lot number, but freshly opened bottle) and ADS PCBM (Amercian Dye Source, Lot#11D030E, purity: >99.0% and Lot#11K022E; purity: >99.0%), labeled A1-PCBM and A2-PCBM. The materials were used as received.

For solar cell preparation, ITO glass substrates (15–20 ohm/square) were cleaned by sonication in toluene, acetone, ethanol, and deionized water sequentially. The substrates were dried under nitrogen and then exposed to UV-ozone for 300 s before spin-coating. The PEDOT:PSS solution (Clevios PVP Al4083) was passed through a 0.45 μm cellulose acetate membrane filter (Toyo Roshi Kaisha, Ltd.) and spin-coated on cleaned substrates at 5000 rpm for 2 min followed by baking the substrate at 120°C for 20 min in a vacuum oven. The active layer was then spin-coated on the top of PEDOT : PSS. For the preparation of the active layer, P3HT and PCBM in a ratio of 1 : 0.8 (27 mg/mL) from different suppliers (American Dye Source P3HT and PCBM, Rieke Metals P3HT, Nano C PCBM) were dissolved in chlorobenzene and stirred separately for 18 h and then mixed together for 2 h at 40°C. The blend solution was spin-coated at 2000 rpm for 1 min. All prepared samples were kept in high vacuum for 2 h and then transferred to Argon filled glove box overnight before evaporating Al electrodes for 100 nm through a shadow mask with 1 mm radius circle. This procedure resulted in devices with the area 3.0 ± 0.3 mm^2 (estimated from 25 devices). Aluminum electrode was used since this is one of the common electrode choices for P3HT : PCBM solar cells.[1,38] Other commonly used electrodes include LiF/Al and Ca/Al,[1] which may have an advantage of improved electron collection selectivity. However, Ca is sensitive to ambient exposure and it is not a convenient electrode choice for an evaporator placed outside a glove box, which is not connected to a glove box. In the case of LiF/Al electrodes, we typically observed an improvement in the fill factor, but a decrease in the short circuit current density for LiF layers, which were as thin as 0.5 nm. It is possible that LiF thickness optimization may yield better results, but this would be difficult to accomplish in existing equipment for such a thin layer (insufficient precision in thickness control).

The devices (R-P3HT : N-PCBM and A1-P3HT : A1-PCBM) were annealed at 130°C (5 min), 140°C (5 min, 15 min) or 150°C (5 min, 15 min), since P3HT with different molecular weight requires different annealing temperatures for optimal performance.[7] On the basis of these data (see Supporting Information), the optimized annealing condition for devices with R-P3HT was chosen to be 150°C for 15 min, while for devices with A1-P3HT the optimum annealing condition was 150°C for 5 min. It should be noted that the annealing time and/or temperature for optimal performance is obviously dependent on the source of P3HT, and thus claims that annealing time should be shorter than 10 min[34] based on only one P3HT : PCBM combination may not necessarily be valid. For example, in other works in the literature annealing time of 30 min has been recommended.[38] On the basis of the number of publications, the most common annealing times are below 20 min, and both pre- and postannealings have been reported.[1] This further confirms that the optimal thermal treatment condition is dependent on the material used, as well as the device preparation procedure.

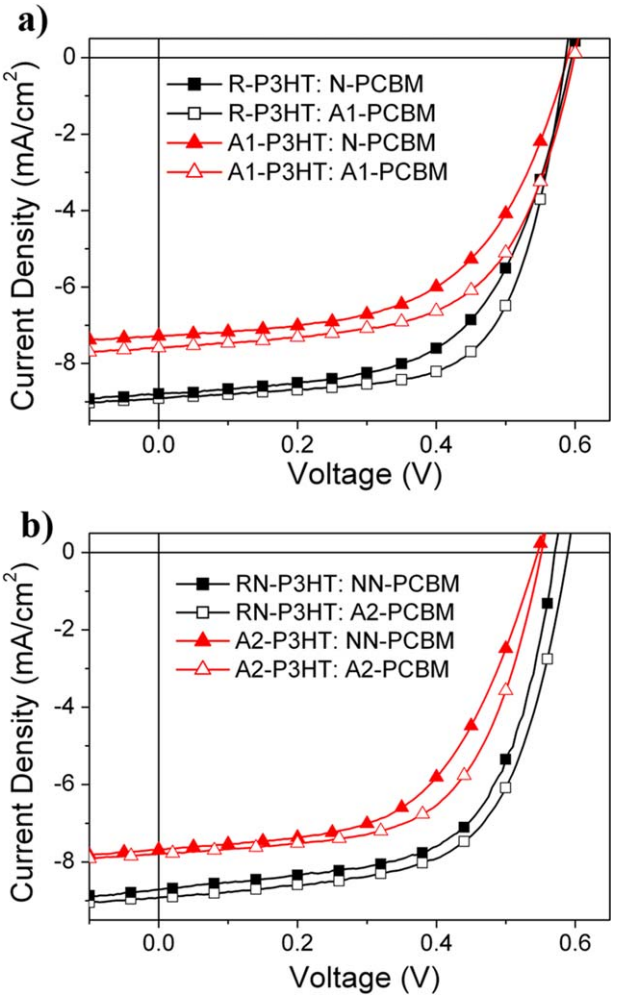

Figure 1. (a, b) I–V curves of solar cells for different combinations of P3HT : PCBM. [Color figure can be viewed in the online issue, which is available at wileyonlinelibrary.com.]

It is thus recommended to test the annealing conditions for each material combination and/or lot number to ensure that the optimal condition is chosen. In our work, annealing times longer than 15 min, resulted in a deterioration of photovoltaic performance.

The I–V characteristics of solar cells were measured by Keithley 2400 sourcemeter under AM 1.5 simulated sunlight illumination (ABET Technologies SUN 2000) at 100 mW/cm^2 (measured by Molectron Power Max 500D laser power meter). Surface morphologies of the samples were characterized by atomic force microscopy (AFM) using Asylum Research MFP3D in semicontact (tapping) mode, at scanning speed of 0.2 Hz using an Olympus AC160TS cantilever. AFM measurements were performed in the area under the Al electrode after removing the electrode using a tape. FTIR measurements were performed using a Perkin Elmer Spectrum Two IR Spectrometer. X-ray diffraction (XRD) patterns were obtained using a Bruker D8 ADVANCE X-ray diffractometer.

RESULTS AND DISCUSSION

Figure 1 shows the I–V curves under AM 1.5 simulated solar illumination for different P3HT : PCBM combinations (corresponding external quantum efficiency (EQE) curves are given in Supporting Information). The performance parameters are summarized in Table I, and they are in the expected range for optimized P3HT : PCBM cells, which typically exhibit short circuit current density $J_{sc} = 8–12$ mA/cm^2 and fill factor $FF = 0.5–0.65$.[1]

It can be observed that the choice of the source material has significant influence on the solar cell performance. This is not surprising, since the P3HT from two sources has different molecular weight and PDI values. The effect of molecular weight on the device performance was studied by different research groups,[4–9] and it was found that there was an optimal $M_{w.}$ [4,5,7] While in some studies higher PDI was found to be favorable for obtaining higher efficiency,[4,7] it was also stated that PDI does not have significant effect on solar cell performance.[1] It should be noted that A1-P3HT and A2-P3HT have very similar M_w but significantly different PDI. However, devices with these two P3HT sources exhibited very similar performance, in agreement with the statement that PDI does not have significant effect on device performance.[1]

A key factor affecting the device performance is the phase separation of the two components in the blend film.[3,37] The short circuit current density is determined by exciton dissociation as well as charge transport and collection, with both charge

Table I. Photovoltaic Parameters for Cells Prepared with Source Material from Different Suppliers

Material	Rms (nm)	V_{oc} (V)	J_s (mA/cm^2)	FF	PCE (%)
R-P3HT : N-PCBM	2.8	0.60 ± 0.01	8.6 ± 0.3 (9.1)	0.60 ± 0.03	3.1 ± 0.2
R-P3HT : A1-PCBM	2.7	0.59 ± 0.01	9.0 ± 0.2 (9.8)	0.64 ± 0.03	3.4 ± 0.2
A1-P3HT : N-PCBM	1.5	0.59 ± 0.01	7.2 ± 0.2 (7.8)	0.56 ± 0.02	2.4 ± 0.2
A1-P3HT : A1-PCBM	1.4	0.60 ± 0.01	7.6 ± 0.3 (8.1)	0.56 ± 0.05	2.6 ± 0.3
RN-P3HT : NN-PCBM	2.4	0.60 ± 0.03	8.6 ± 0.3 (8.6)	0.63 ± 0.02	3.3 ± 0.2
RN-P3HT : A2-PCBM	3.0	0.59 ± 0.004	9.1 ± 0.2 (9.8)	0.62 ± 0.01	3.4 ± 0.1
A2-P3HT : NN-PCBM	1.4	0.57 ± 0.04	7.5 ± 0.2 (7.5)	0.57 ± 0.05	2.4 ± 0.3
A2-P3HT : A2-PCBM	2.0	0.58 ± 0.02	7.9 ± 0.2 (8.2)	0.56 ± 0.03	2.5 ± 0.2

The average values and errors were determined for 12 devices. The short circuit current density estimate obtained from EQE is given in brackets (see Supporting Information for the description of estimating procedure).

Applied Polymer SCIENCE

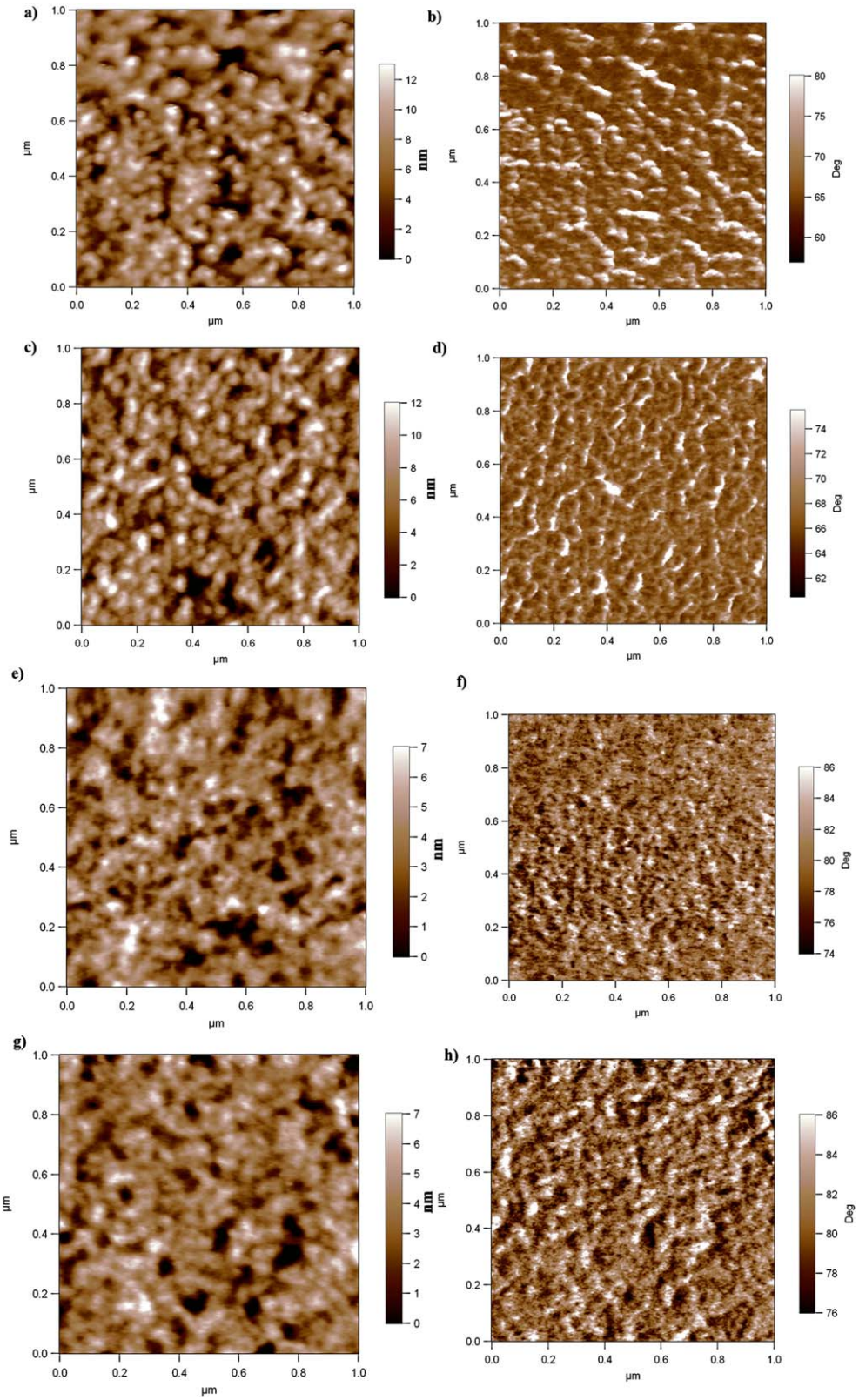

Figure 2. Topography (left) and phase (right) AFM images for (a), (b) R-P3HT : N-PCBM; (c, d) R-P3HT : A1-PCBM; (e, f) Al-P3HT : N-PCBM; (g, h) A1-P3HT : A1-PCBM. [Color figure can be viewed in the online issue, which is available at wileyonlinelibrary.com.]

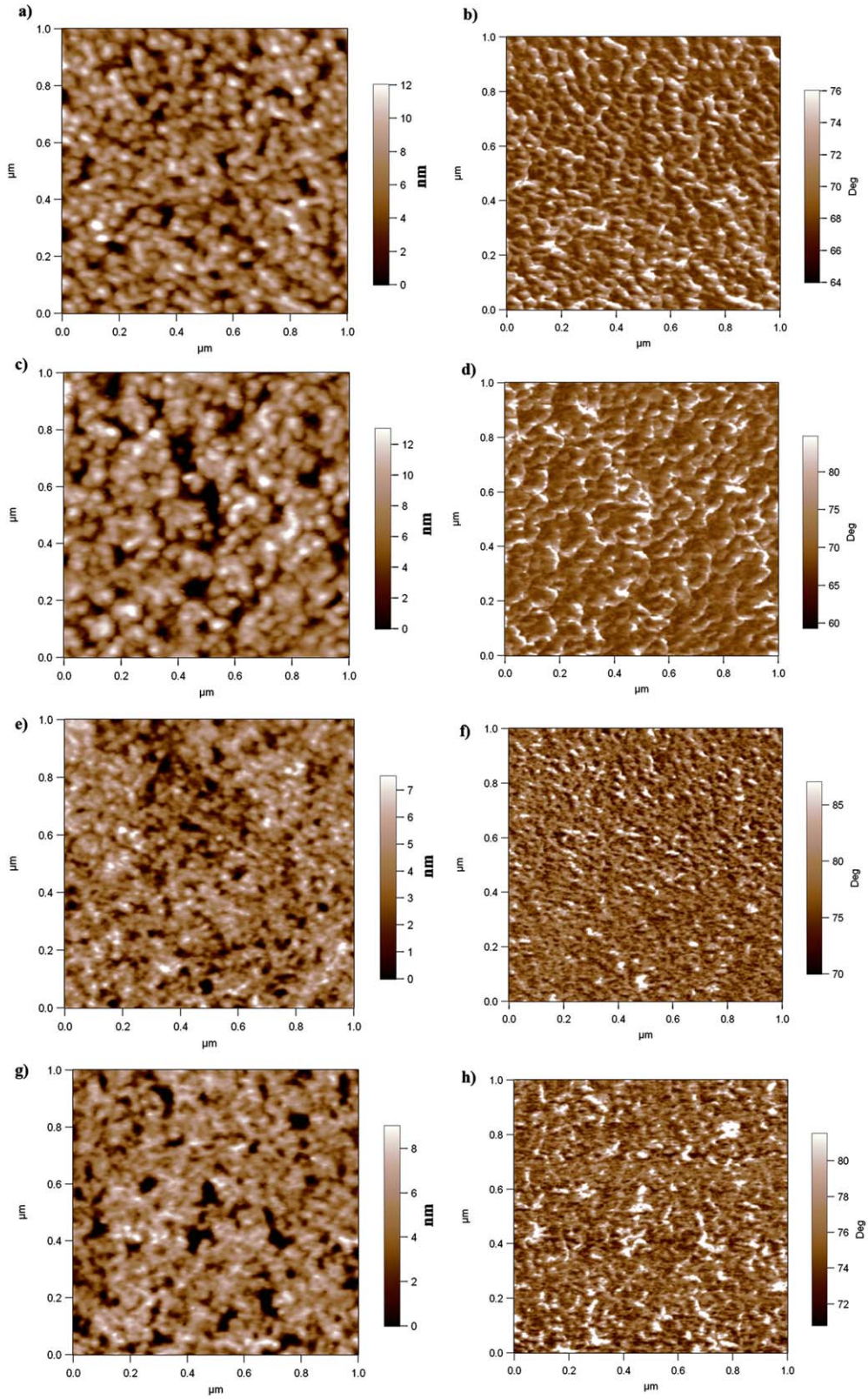

Figure 3. Topography (left) and phase (right) AFM images for (a), (b) RN-P3HT : NN-PCBM; (c, d) RN-P3HT : A2-PCBM; (e, f) A2-P3HT : NN-PCBM; (g, h) A2-P3HT : A2-PCBM. [Color figure can be viewed in the online issue, which is available at wileyonlinelibrary.com.]

Applied Polymer SCIENCE

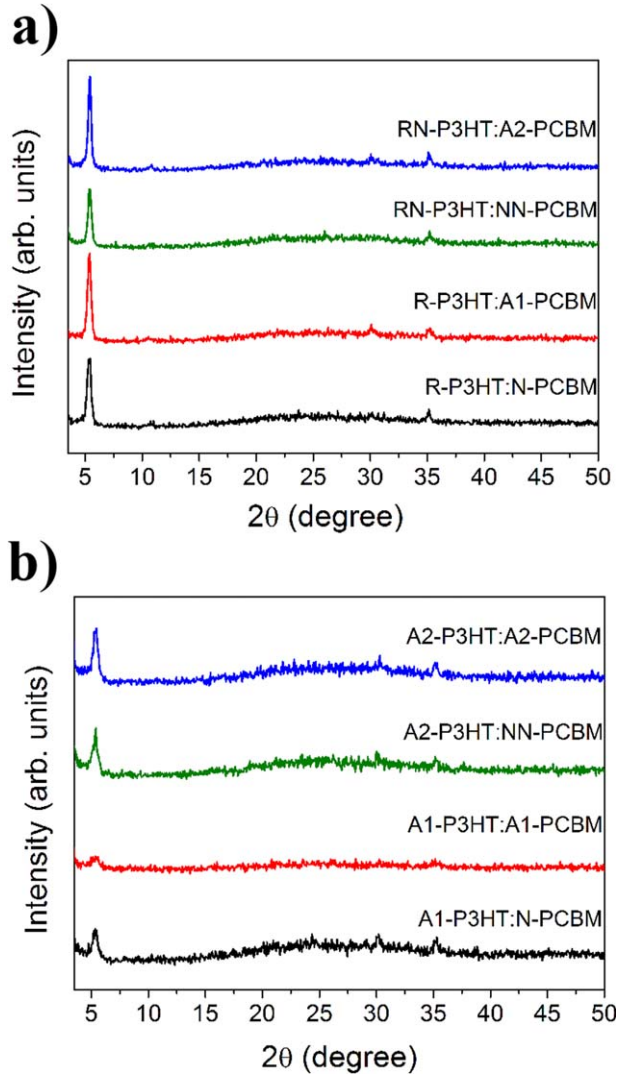

Figure 4. XRD patterns of P3HT : PCBM blend films for (a) R-P3HT and RN-P3HT, (b) A1-P3HT, and A2-P3HT. [Color figure can be viewed in the online issue, which is available at wileyonlinelibrary.com.]

generation and charge collection processes being dependent on the blend film morphology.[3] We can observe that there is a significant variation in the short circuit current density for cells prepared with different source materials, from 7.2 to 9.1 mA/cm^2. Fill factor is also affected by the phase separation, as well as the recombination mechanisms in the device.[3] Devices exhibiting lower photocurrents ($J_{sc} < 8.0$ mA/cm^2) in our work also exhibit lower *FF* values (<0.60). While the maximum open circuit voltage V_{oc} is determined by the difference of the HOMO and LUMO levels of the polymer and PCBM, in practice it typically has a complex relationship with the properties of the bulk heterojunction as well as electrode interfaces.[3] The variations of V_{oc} we have observed among the devices have been small, unlike the differences in the *FF* and J_{sc}. Since these two photovoltaic performance parameters are strongly dependent on the blend film properties, we have investigated the properties of blend films for different combinations of P3HT and PCBM. Obtained AFM images (topography and phase contrast) are shown in Figures 2 and 3, respectively. XRD patterns are shown in Figure 4. We can observe that the samples exhibit different surface roughness as well as differences in phase separation (domain sizes and shapes). Lower efficiency devices (those prepared with A1-P3HT and A2-P3HT) generally exhibit finer mixing of P3HT and PCBM, which is likely less favorable for charge transport and extraction, resulting in lower J_{sc} and *FF* values. Lower efficiency devices also exhibited inferior P3HT crystallinity, as can be observed from Figure 4 and estimated crystallite size (Table SIV, Supporting Information), which is expected since improved crystallinity (together with favorable phase separation) results in increased power conversion efficiency.[37] Surprisingly, not only the P3HT used affected the morphology and performance, but also PCBM had some effect as well. For the same P3HT material used, the choice of PCBM affected P3HT crystallinity and consequently affected the photovoltaic performance. Furthermore, the two sources of PCBM had a difference in sample purity (99.5% for N- and NN-PCBM, >99% for A1- and A2-PCBM). Various impurities present in the starting materials can serve as recombination sites and affect the charge transport in the blend film.[1] Thus, we decided to examine the source material using FTIR. Obtained spectra for P3HT and PCBM are shown in Figures 5 and 6, respectively (blend film characterization results are summarized in Table SIV, Supporting Information).

FTIR spectra of P3HT and/or PCBM have been reported previously,[41–46] and the data obtained here are in good agreement with previous reports. Because of the differences in the presence of broad peak at ~3400–3600 cm^{-1}, which can be attributed to the presence of hydroxyl groups and water, we have also exposed fresh P3HT and PCBM to ambient air for ~60 h, and those samples are labeled as NNA-PCBM, A2A-PCBM, RNA-P3HT, and A2A-P3HT. We can observe that samples from American Dye Source appear to be more sensitive to ambient exposure, judging from more prominent dips corresponding to samples exposed to ambient air, as well as samples stored in a dry cabinet (samples A1-PCBM, A1-P3HT, N-PCBM, and R-P3HT were stored in a dry cabinet for several weeks to several months before use). However, increased presence of water impurities does not necessarily have detrimental effect on solar cell performance, as can be observed from the data in Table I. For P3HT, the peaks at ~2955 and 2925 belong to the C—H stretching vibrations [41,44] ~2856 cm^{-1} feature is due to stretching of —CH_2—[44] while band at ~1376 cm^{-1} belongs to the stretching vibration of the thiophene ring.[41] Here we have not observed any prominent peaks at ~1260 cm^{-1} (another stretching vibration of the thiophene ring) or ~1063 cm^{-1} (stretching vibration of C—O group due to oxidation of P3HT).[41] The peak at ~1510 cm^{-1} corresponds to asymmetric C=C stretching vibration,[42] while the peak at ~1460 cm^{-1} is due to symmetric C=C stretching vibration.[46] An increase in the intensity ratios of asymmetric and symmetric C=C stretching vibrations is typically observed with increased conjugation length[42,46] Ratios of the peak intensities at 1510 and 1456 cm^{-1} was slightly higher for A1-P3HT and A2-P3HT (1.16 and 1.17, respectively) as compared to R-P3HT and RN-P3HT (1.03 and 1.08), indicating somewhat longer conjugation length. The feature at ~720 cm^{-1} corresponds to rocking vibration of —

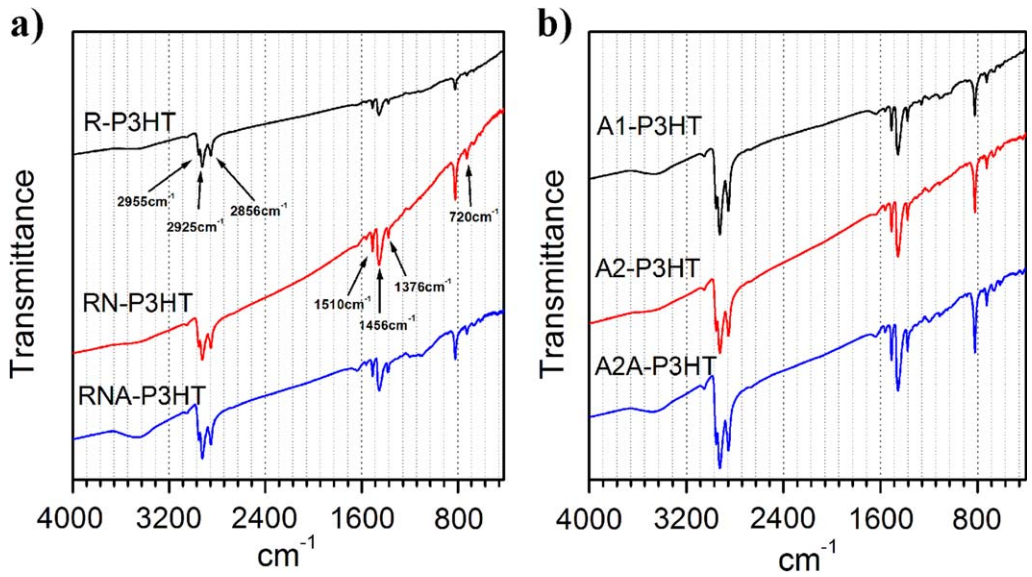

Figure 5. FTIR spectra for different sources of P3HT. [Color figure can be viewed in the online issue, which is available at wileyonlinelibrary.com.]

$(CH_2)_n$— group.[43] In PCBM spectra, the feature at ~1740 cm^{-1} is due to C═O group, while the peaks at ~520 cm^{-1}, ~570 cm^{-1}, ~1180 cm^{-1}, ~1450 cm^{-1} correspond to fullerene.[45] For both P3HT and PCBM, the most pronounced difference in the spectra of materials obtained from different suppliers is the presence of water, which becomes more pronounced with PCBM from American Dye Source being more sensitive to ambient air exposure.

The most significant parameter affecting the blend film properties and photovoltaic performance appears to be the molecular weight of P3HT, although the source (and possibly purity) of PCBM also affect the blend film morphology, crystallinity, and photovoltaic performance although to a smaller degree as compared to P3HT. This is likely because both factors can affect the diffusion of PCBM during annealing and thus final morphology of the blend film. It should be noted however that AFM examination only reveals morphological differences at the top surface. Device performance is strongly affected by the variation in the blend film morphology as well as interfacial behavior (preferential segregation of one component at the interfaces).[3] The reported gradients of phase separation of P3HT : PCBM (enrichment of P3HT or PCBM at film/air interface) in the literature have been contradictory, with different studies reporting favorable (PCBM) or unfavorable (P3HT) enrichment at the top surface of the film.[3] It should be noted that the differences in reported literature could occur due to differences in device processing techniques as well as device architecture from one study to another. To examine the possibility of differences in

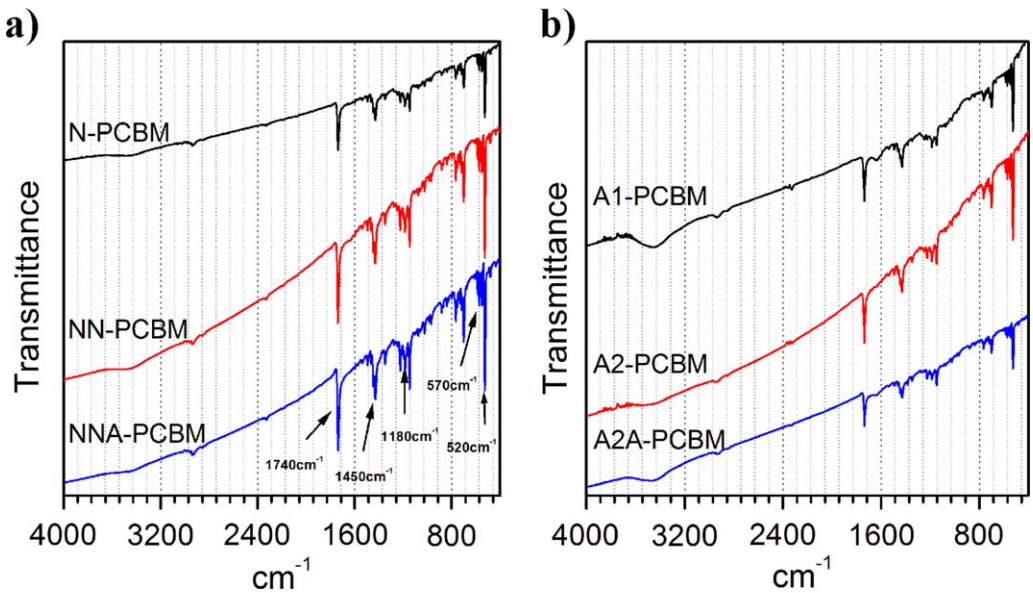

Figure 6. FTIR spectra for different sources of PCBM. [Color figure can be viewed in the online issue, which is available at wileyonlinelibrary.com.]

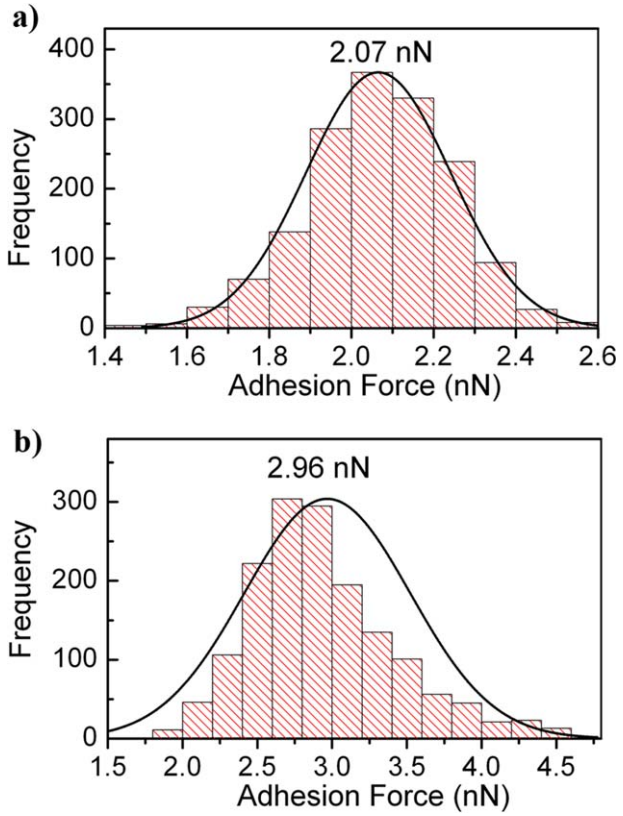

Figure 7. Histograms of adhesion force of (a) RN-P3HT : NN-PCBM and (b) A2-P3HT : NN-PCBM blend films. [Color figure can be viewed in the online issue, which is available at wileyonlinelibrary.com.]

gradient of phase separation among devices, the composition of the sample surface was examined by XPS and presence of sulfur was compared (see Supporting information). No significant differences were obtained for the two sources of P3HT and no significant correlation with device performance was found, indicating that the main contributing factor to the different photovoltaic performance is the different morphology of the blend film (in terms of roughness and size of the domains).

In addition to the differences in device performance, bulk heterojunctions prepared using P3HT and PCBM from different suppliers also exhibit other differences. For example, delamination of the Al electrode[38] can be easily achieved in blends with R- and RN- P3HT, while it is difficult to remove the cathode for blends with A1- and A2- P3HT. Furthermore, for devices with R- and RN-P3HT, spin-coating of PCBM from DCM solutions on top of the blend layer resulted in worsening of the film quality (significant coarsening and partial delamination) and consequently worsening of the device performance, while for A1- and A2- P3HT no worsening of the film quality occurred and device performance improved (see Supporting information for device photos and AFM images).[36] Spin-coating of PCBM from DCM solution is sometimes used in P3HT/PCBM bilayer, as well as bulk heterojunction devices, to achieve favorable intermixing of P3HT and PCBM, with PCBM-rich domains at the top surface.[47,48] To examine this in more detail, adhesion force mapping was performed by AFM.[49] Adhesion force between the tip and sample is obtained from the retracted part of the force-distance curve determined by AFM characterization.[50] Obtained results are shown in Figure 7. It can be observed that significantly higher adhesion forces are obtained for a blend film containing A2-P3HT as compared to RN-P3HT. This is in agreement with the observation that RN-P3HT blends are damaged by spin-coating PCBM on the top, as well as the fact that Al electrode can be easily peeled off. This indicates that P3HT samples with lower molecular weight may be less suitable for the preparation of multilayer devices and tandem cells, and they may also have worse stability since it would be easier for Al electrode to separate from the blend film.

CONCLUSIONS

We have studied the influence of P3HT and PCBM from different suppliers on the blend film properties and photovoltaic performance. We found that the P3HT properties had significant effect on blend film adhesion and optimal annealing conditions, while both P3HT and PCBM properties affected the blend film morphology and photovoltaic performance. Samples with lower molecular weight exhibited lower adhesion, which has implications on fabrication of multilayer devices and long term device stability.

ACKNOWLEDGEMENTS

This work was supported by the Strategic Research Theme and University Development Fund, (administrated by The University of Hong Kong) and ITP/038/10NP grant from the Innovation and Technology Commission of the Hong Kong government. The authors would like to thank Hong Kong Science Park for XPS measurements.

REFERENCES

1. Dang, M. T.; Hirsch, L.; Wantz, G. *Adv. Mater.* **2011**, *23*, 3597.
2. Li, G.; Shrotriya, V.; Yao, Y.; Huang, J.; Yang, Y. *J. Mater. Chem.* **2007**, *17*, 3126.
3. Brady, M. A.; Su, G. M.; Chabinyc, M. L. *Soft Matter* **2011**, *7*, 11065.
4. Kim, Y. S.; Lee, Y.; Lee, W.; Park, H.; Han, S. H.; Lee, S. H. *Curr. Appl. Phys.* **2010**, *10*, 329.
5. Ma, W.; Kim, J. Y.; Lee, K.; Heeger, A. *J. Macromol. Rapid Commun.* **2007**, *28*, 1776.
6. Schilinsky, P.; Asawapirom, U.; Scherf, U.; Biele, M.; Brabec, C. *J. Chem. Mater.* **2005**, *17*, 2175.
7. Hiorns, R. C.; de Bettignies, R.; Leroy, J.; Bailly, S.; Firon, M.; Sentein, C.; Preud'homme, H.; Dagron-Lartigau, C. *Eur. Phys. J. Appl. Phys.* **2006**, *36*, 295.
8. Nicolet, C.; Deribew, D.; Renaud, C.; Fleury, G.; Brochon, C.; Cloutet, E.; Vignau, L.; Wantz, G.; Cramail, H.; Geoghegan, M.; Hadziioannou, G. *J. Phys. Chem. B.* **2011**, *115*, 12717.
9. Ballantyne, A. M.; Chen, L.; Dane, J.; Hammant, T.; Braun, F. M.; Heeney, M.; Duffy, W.; McCulloch, I.; Bradley, D. D. C.; Nelson, *J. Adv. Funct. Mater.* **2008**, *18*, 2373.

10. Rice, A. H.; Giridharagopal, R.; Zheng, S. X.; Ohuchi, F. S.; Ginger, D. S.; Luscombe, C. K. *ACS Nano* **2011**, *5*, 3132.
11. Wang, W. L.; Wu, H. B.; Yang, C. Y.; Luo, C.; Zhang, Y.; Chen, J. W.; Chao, Y. *Appl. Phys. Lett.* **2007**, *90*, 1835121.
12. Li, L. G.; Lu, G. H.; Yang, X. N. *J. Mater. Chem.* **2008**, *18*, 1984.
13. Chen, D.; Nakahara, A.; Wei, D. G.; Nordlund, D.; Russell, T. P. *Nano Lett.* **2011**, *11*, 561.
14. Wu, W. R.; Jeng, U. S.; Su, C. J.; Wei, K. H.; Su, M. S.; Chiu, M. Y.; Chen, C. Y.; Su, W. B.; Su, C. H.; Su, A. C. *ACS Nano* **2011**, *5*, 6233.
15. Turner, S. T.; Pingel, P.; Steyrleuthner, R.; Crossland, E. J. W.; Ludwigs, S.; Neher, D. *Adv. Funct. Mater.* **2011**, *21*, 4640.
16. Collins, B. A.; Tumbleston, J. R.; Ade, H. *J. Phys. Chem. Lett.* **2011**, *2*, 3135.
17. Yang, Y.; Lee, K.; Mielczarek, K.; Hu, W.; Zakhidov, A. *Nanotechnology* **2011**, *22*, 4853011.
18. Dang, M. T.; Wantz, G.; Bejbouji, H.; Urien, M.; Dautel, O. J.; Vignau, L.; Hirsch, L. *Sol. Energy Mater. Sol. Cells* **2011**, *95*, 3408.
19. Park, B.; Huh, Y. H.; Shin, J. C. *Sol. Energy Mater. Sol. Cells* **2011**, *95*, 3543.
20. Fan, X.; Fang, G. J.; Qin, P. L.; Cheng, F.; Zhao, X. Z. *Appl. Phys. A* **2011**, *105*, 1003.
21. Chen, S. Y.; Yen, Y. T.; Chen, Y. Y.; Hsu, C. S.; Chueh, Y. L.; Chen, L. *J. RSC Adv.* **2012**, *2*, 1314.
22. Huang, L. C.; Liu, H. W.; Liang, C. W.; Chou, T. R.; Wang, L.; Chao, C. Y. *Soft Matter* **2012**, *8*, 1467.
23. Liu, Z. H.; Lee, E. C. *J. Appl. Phys.* **2012**, *111*, 0231041.
24. Bagui, A.; Iyer, S. S. K. *IEEE Trans. Electron Devices* **2011**, *58*, 4061.
25. Baek, W. H.; Yang, H.; Yoon, T. S.; Kang, C. J.; Lee, H. H.; Kim, Y. S. *Sol. Energy Mater. Sol. Cells* **2009**, *93*, 1263.
26. Wang, T.; Pearson, A. J.; Lidzey, D. G.; Jones, R. A. L. *Adv. Funct. Mater.* **2011**, *21*, 1383.
27. Zhang, C. F.; Hao, Y.; Tong, S. W.; Lin, Z. H.; Feng, Q. A.; Kang, E. T.; Zhu, C. X. *IEEE Trans. Electron Devices* **2011**, *58*, 835.
28. Keawprajak, A.; Piyakulawat, P.; Klamchuen, A.; Iamraksa, P.; Asawapirom, U. *Sol. Energy Mater. Sol. Cells* **2010**, *94*, 531.
29. Peng, B.; Guo, X.; Cui, C. H.; Zou, Y. P.; Pan, C. Y.; Li, Y. F. *Appl. Phys. Lett.* **2011**, *98*, 2433081.
30. Chen, D.; Liu, F.; Wang, C.; Nakahara, A.; Russell, T. P. *Nano Lett.* **2011**, *11*, 2071.
31. Reyes-Reyes, M.; Kim, K.; Carroll, D. L. *Appl. Phys. Lett.* **2005**, *87*, 0835061.
32. Kim, K.; Liu, J.; Namboothiry, M. A. G.; Carroll, D. L. *Appl. Phys. Lett.* **2007**, *90*, 1635111.
33. Yao, Y.; Hou, J. H.; Xu, Z.; Li, G.; Yang, Y. *Adv. Funct. Mater.* **2008**, *18*, 1783.
34. Treat, N. D.; Shuttle, C. G.; Toney, M. F.; Hawker, C. J.; Chabinyc, M. L. *J. Mater. Chem.* **2011**, *21*, 15224.
35. Xiao, T.; Cui, W.; Anderegg, J.; Shinar, J.; Shinar, R. *Org. Electron.* **2011**, *12*, 257.
36. Ng, A.; Sun, Y. C.; Fung, M. K.; Ng, A. M. C.; Leung, Y. H.; Djurišić, A. B.; Chan, W. K. *Proc. SPIE* **2012**, *8258*, 82581E1.
37. Yang, X. N.; Loos, J.; Veenstra, S. C.; Verhees, W. J. H.; Wienk, M. M.; Kroon, J. M.; Michels, M. A. J.; Janssen, R. A. *J. Nano Lett.* **2005**, *5*, 579.
38. Ma, W. L.; Xang, C. Y.; Gong, X.; Lee, K. H.; Heeger, A. *J. Adv. Funct. Mater.* **2005**, *15*, 1617.
39. Tsai, J. H.; Lai, Y. C.; Higashihara, T.; Lin, C. J.; Ueda, M.; Chen, W. C. *Macromolecules* **2010**, *43*, 6085.
40. Kim, Y. K.; Cook, S.; Tuladhar, S. M.; Choulis, S. A.; Nelson, J.; Durrant, J. R.; Bradley, D. D. C.; Giles, M.; McCulloch, I.; Ha, C. S.; Ree, M. *Nature Mater.* **2006**, *5*, 197.
41. Xu, S. B.; Gu, L. X.; Wu, K. H.; Yang, H. G.; Song, Y. Q.; Jiang, L.; Dan, Y. *Sol. Energy Mater. Sol. Cells* **2012**, *96*, 286.
42. Trznadel, M.; Pron, A.; Zagorska, M.; Chrzaszcz, R.; Pielichowski, *J. Macromolecules* **1998**, *31*, 5051.
43. Koizhaiganova, R.; Kim, H. J.; Vasudevan, T.; Kudaibergenov, S.; Lee, M. S. *J. Appl. Polym. Sci.* **2010**, *115*, 2448.
44. Gholamkhass, B.; Holdcroft, S. *Chem. Mater.* **2010**, *22*, 5371.
45. Peng, F. G.; Wu, J. H.; Li, Q. B.; Wang, Y.; Yue, G. T.; Xiao, Y. M.; Li, Q. H.; Lan, Z.; Fan, L. Q.; Lin, J. M.; Huang, M. L. *Electrochim. Acta* **2011**, *56*, 5184.
46. Kim, K.; Shin, J. W.; Lee, Y. B.; Cho, M. Y.; Lee, S. H.; Park, D. H.; Jang, D. K.; Lee, C. J.; Joo, *J. ACS Nano* **2010**, *4*, 4197.
47. De Villers, B. T.; Tassone, C. J.; Tolbert, S. H.; Schwartz, B. J. *J. Phys. Chem. C* **2009**, *113*, 18978.
48. Ayzner, A. L.; Tassone, C. J.; Tolbert, S. H.; Schwartz, B. J. *J. Phys. Chem. C* **2009**, *113*, 20050.
49. Eaton, P.; Smith, J. R.; Graham, P.; Smart, J. D.; Nevell, T. G.; Tsiboukis, *J. Langmuir* **2002**, *18*, 3387.
50. Li, X. J.; Chen, W.; Zhan, Q. W.; Dai, L. M.; Sowards, L.; Pender, M.; Naik, R. R. *J. Phys. Chem. B* **2006**, *110*, 12621.